Brought to you by:
Korea University Library

Login: ⊞
Register

Home | Browse | Search | My Settings | Alerts | Help

Quick Search
search tips

All fields
Author
Journal/book title
Volume
Issue
Page

Clear ⊗   Go ➔   Advanced Search

Font Size: ➖ ➕

Article | Figures/Tables | References | 📄 PDF (705 K)

Thumbnails | Full-Size Images

doi:10.1016/j.synthmet.2009.08.009
❓ Cite or Link Using DOI

Photoreactive main chain conjugated polymer containing oxetane moieties in the side chain and its application to green electrophosphorescence devices

Min Ju Cho[a], Jicheol Shin[a], Jung-Il Jin[a], Young Min Kim[b], Young Wook Park[b], Byeong-Kwon Ju[b] and Dong Hoon Choi[a], 📝, ✉️

[a]Department of Chemistry, Advanced Materials Chemistry Research Center, Korea University, 5 Anam-dong, Sungbuk-gu, Seoul 136-701, Republic of Korea
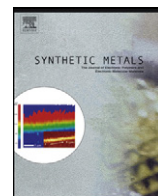
[b]Display and Nanosystem Laboratory, College of Engineering, Korea University, 5 Anam-dong, Sungbuk-gu, Seoul 136-701, Republic of Korea

Article Toolbox

✉️ E-mail Article   📋 Export Citation
❝ Cited By   Add to my Quick Links
▶ Save as Citation Alert   Permissions & Reprints
📡 Citation Feed   Cited By in Scopus (0)

Related Articles in ScienceDirect

- Hole injection and transport in ITO/PEDOT/PVK/Al diodes
  Materials Science and Engineering: C
- Effects of solution-processed polymer interlayers on ho...
  Organic Electronics
- Blue light-emitting, electron-transporting materials ba...
  Chemical Physics Letters
- A soluble self-doped conducting polyaniline graft copol...

Photoreactive main chain conjugated polymer containing oxetane moieties in the side chain and its application to green electrophosphorescence devices

Min Ju Cho[a], Jicheol Shin[a], Jung-Il Jin[a], Young Min Kim[b], Young Wook Park[b], Byeong-Kwon Ju[b], Dong Hoon Choi[a,*]

[a] Department of Chemistry, Advanced Materials Chemistry Research Center, Korea University, 5 Anam-dong, Sungbuk-gu, Seoul 136-701, Republic of Korea
[b] Display and Nanosystem Laboratory, College of Engineering, Korea University, 5 Anam-dong, Sungbuk-gu, Seoul 136-701, Republic of Korea

ABSTRACT

The utilization of a photoreactive hole injection/transport layer in multilayer electrophosphorescence polymer light-emitting diodes (PLEDs) is demonstrated in this study. A new photoreactive polymer was synthesized using 3,6-dibromo-9-(6-((3-methyloxetan-3-yl)methoxy)hexyl)-9H-carbazole and 2,4-dimethyl-N,N-bis(4-(4,4,5,5-tetramethyl-1,3,2-dioxaborolan-2-yl)phenyl)aniline *via* the Suzuki coupling reaction. When oxetane groups were photopolymerized in the presence of a cationic photoinitiator, the cured film showed good compatibility with PEDOT:PSS and the indium tin oxide (ITO) layer due to the hydrophilic nature of the cross-linked section. The resulting green light-emitting device bearing PVK:PBD:Ir(Cz-ppy)$_3$ exhibits a maximum external quantum efficiency of 8.73%, corresponding to a luminous efficiency of 28.2 cd/A when using the device configuration of ITO/POx-TPACz/PEDOT:PSS/PVK:PBD:Ir(Cz-ppy)$_3$/TAZ/Alq$_3$/LiF/Al. These values are higher than those of PLEDs using conventional PEDOT:PSS as a single hole injection layer (HIL). The slight degree of improvement in device efficiency is due to the reduced hole injection barrier.

© 2009 Elsevier B.V. All rights reserved.

1. Introduction

Of the various light-emitting organic materials available, phosphorescent dye molecules are particularly promising because both singlet and triplet excitons can generate unique light emission with a theoretical internal quantum efficiency of 100% [1–3]. In particular, cyclometalated Ir(III) complexes show high phosphorescent efficiencies and are one of the most important classes of phosphorescent dyes [4–9]. When preparing electrophosphorescence devices, the multilayered device configuration is usually designed employing various auxiliary carrier transport and blocking layers to improve device efficiency. Among the various auxiliary layers, the hole injection/transporting layer (HIL/HTL) most significantly affects the multilayer device performance of polymer light-emitting diodes (PLEDs). It controls the efficiency of hole injection and transport from the anode into a light-emitting layer (EML). The interfacial contact between ITO/HIL or HIL/HTL particularly limits charge injection and transport [10–13].

When developing highly efficient multilayer PLEDs, it is desirable to develop robust hole transporting materials that possess an energy level that corresponds with the indium tin oxide (ITO) anode and the highest occupied molecular orbital (HOMO) of the light-emitting material to facilitate efficient hole injection and transport. In order to fabricate the device *via* solution processing, the HIL or HTL material must possess good solvent resistance and compatibility with the other layers.

In green electrophosphorescent PLEDs, large bandgap host materials, such as poly(N-vinylcarbazole), polyfluorene, etc., with triplet energy higher than that of the phosphorescent Ir(III) complex should be employed to avoid back energy transfer from the Ir(III) complex to the host polymer. Because of the high HOMO energy level of these large bandgap polymers (e.g., E_g^{PVK} is ∼3.6 eV; E_{HOMO}^{PVK} is usually greater than 5.6 eV), the efficiency of the hole injection from ITO to the EML can be suppressed if only a single HIL is employed in the device. Therefore, additional HTL (or HIL) is combined with conventional HIL to form a facile cascade energy profile for achieving efficient hole injection and charge confinement. For fabricating multilayered devices solely by solution processing, either photo- or thermally cross-linked hole transporting materials are frequently employed [14–22]. In addition, for improving the compatibility of poly(3,4-ethylenedioxythiophene)/(polystyrene sulfonate) (PEDOT/PEDOT:PSS) with conventional hole transporting materials, it is necessary to design HIL or HTL materials having a hydrophilic nature after the photo- or thermal-curing process.

---

* Corresponding author. Tel.: +82 2 3290 3140; fax: +82 2 924 3141.
  E-mail address: dhchoi8803@korea.ac.kr (D.H. Choi).

This paper describes the synthesis of a new photoreactive polymer (POx-TPACz) bearing oxetane moieties in the side chain. This polymer was employed as a hole injecting or transporting material in multilayer electrophosphorescence PLEDs. Several devices were prepared with different configurations and their performances were compared. In one device, the POx-TPACz was replaced with PEDOT:PSS. In two different devices, the photoreactive polymer layer was employed, not only for the hole injection layer on the ITO anode, but also for the hole transporting layer on PEDOT:PSS. A highly soluble Ir(III) complex, Ir(Cz-ppy)$_3$ bearing a carbazolyl-substituted 2-phenylpyridine ligand was used as the green emitting dopant, and a nonconjugated polymer [23], PVK was used as the host in this study.

In order to improve the charge transport balance, 30% 5-4-*tert*-butylphenyl-1,3,4-oxadiazole (PBD) was doped in PVK as an electron transport molecule. The emission center in Ir(Cz-ppy)$_3$ was observed to be fairly isolated and its properties were not much affected by the presence of a carbazolyl peripheral group. The function of an interlayer of POx-TPACz was investigated in terms of the device efficiency of electrophosphorescent PLEDs.

2. Experimental

2.1. Synthesis

Compounds **2** and **4** were synthesized by following the literature method [24,25].

2.1.1. 3,6-Dibromo-9-(6-((3-methyloxetan-3-yl)methoxy)hexyl)-9H-carbazole (3)

Sodium hydride (1.2 g, 23 mmol, 55% suspension in mineral oil) was suspended in dried dimethylformamide (DMF, 100 mL) at 0 °C. 3,6-Dibromo-9H-carbazole (7.0 g, 21 mmol) in DMF (50 mL) was added dropwise into the mother solution and stirred for 1 h. Then, 3-((6-bromohexyloxy)methyl)-3-methyloxetane (5.71 g, 21 mmol) in DMF (50 mL) was also added dropwise over a 30 min period and the reaction mixture was kept stirring at room temperature for 12 h. After completion of the reaction, the solution was extracted with ethylacetate/water and its organic layer was dried under Na$_2$SO$_4$. The dried solution was concentrated. The resulting crude oily product was purified by silica gel column chromatography (ethylacetate:hexane = 1:3) to yield 7.3 g (66%) of white powder.

^{1}H NMR (400 MHz, CDCl$_3$): δ (ppm) 8.14 (d, J = 2.4 Hz, 2H), 7.55 (dd, J_1 = 2.4 Hz, J_2 = 8.4 Hz, 2H), 7.27 (d, J = 8.4 Hz, 2H), 4.47 (d, 2H), 4.33 (d, 2H), 4.24 (t, 2H), 3.37–3.42 (m, 4H), 1.78–1.88 (m, 2H), 1.48–1.56 (m, 2H), 1.33–1.39 (m, 4H), 1.27 (s, 3H).

2.1.2. Suzuki coupling polymerization (5)

A solution of 3,6-dibromo-9-(6-((3-methyloxetan-3-yl)methoxy)hexyl)-9H-carbazole, **3** (1.53 g, 3.0 mmol), 2,4-dimethyl-*N,N*-bis(4-(4,4,5,5-tetramethyl-1,3,2-dioxaborolan-2-yl)phenyl)aniline, **4** (1.58 g, 3.0 mmol), Pd(PPh$_3$)$_4$ (0.069 g, 0.06 mmol), and aliquat 336 (0.5 g) in a mixture of toluene (25 mL) and aqueous 2 M K$_2$CO$_3$ (15 mL) was refluxed with vigorous stirring 36 h under argon gas. The cooled mixture was poured into methanol (200 mL) and the precipitate was recovered by filtration. Purification of polymer by soxhlet extraction with methanol for 24 h afforded white solid **5** in 85% yield.

^{1}H NMR (400 MHz, CDCl$_3$): δ (ppm) 8.30 (s, 2H), 7.67 (m, 2H), 7.57 (m, 4H), 7.41 (m, 2H), 7.11 (m, 7H), 4.46 (m, 2H), 4.31 (m, 4H), 3.40 (m, 4H), 2.35 (s, 3H), 2.10 (s, 3H), 1.90 (m, 2H), 1.54 (m, 2H), 1.40 (m, 4H), 1.26 (s, 3H). GPC (THF): Weight-average molecular weight M_w = 7500 g mol^{-1}, number-average molecular weight M_n = 4300 g mol^{-1}.

2.2. Instrumental analysis

^{1}H NMR spectra were recorded on a Varian Mercury NMR 400 MHz spectrometer using deuterated chloroform (CDCl$_3$) purchased from Cambridge Isotope Laboratories, Inc. Molecular weight of the polymer, POx-TPACz was determined by gel permeation chromatography (GPC, Waters) using polystyrene as a standard and THF as an eluent.

Thermal properties were studied under a nitrogen atmosphere on a Mettler DSC 821e instrument. Thermal gravimetric analysis (TGA) was conducted on a Mettler TGA50 thermal analysis system under a heating rate of 10 °C/min.

Absorption spectrum of chloroform solution was obtained using a UV–vis spectrometer (HP 8453, PDA type) in the wavelength range of 190–1100 nm. In order to prepare the film sample, the POx-TPACz was dissolved in monochlorobenzene, 2 wt.% of the cationic photoinitiator, [4-[(2-hydroxytetradecyl)oxy]-phenyl]phenyliodonium hexafluoroantimonate was added and finally the solution was spin-coated on a quartz glass. The films were exposed to UV-light (λ_{max} = 254 nm, intensity = 40 mW/cm^2) for 120 s at 150–160 °C. In order to investigate the solvent resistivity by using UV–vis absorption spectroscopy, the exposed films were rinsed using monochlorobenzene as a solvent and the spectrum was taken again.

2.3. Electroluminescence measurement

The multilayer diodes have a structure of ITO/(HIL and/or HTL)/PVK:PBD with Ir(III) complex (40 nm)/TAZ (10 nm)/Alq$_3$ (30 nm)/LiF (0.8 nm)/Al (80 nm), respectively. Generally, in Device A, the conducting PEDOT:PSS layer was spin-coated onto the ITO-coated glasses in an argon atmosphere. The emitting PVK/Ir-complex layer then was spin-coated onto the thoroughly dried PEDOT:PSS layer using the solution (conc.: 1.5 wt.%) in monochlorobenzene. In the other devices, the POx-TPACz solution in monochlorobenzene was spin-coated on ITO or PEDOT:PSS layer and the polymer layer was exposed to the UV light (λ = 254 nm, I = 40 mW/cm^2 for 150–160 °C, 120 s).

Four device configurations are as follows:

Device A: ITO/PEDOT:PSS/PVK:PBD:Ir(Cz-ppy)$_3$/TAZ/Alq$_3$/Lif/Al,
Device B: ITO/PEDOT:PSS/POx-TPACz/PVK:PBD:Ir(Cz-ppy)$_3$/TAZ/Alq$_3$/Lif/Al,
Device C: ITO/POx-TPACz/PVK:PBD:Ir(Cz-ppy)$_3$/TAZ/Alq$_3$/Lif/Al,
Device D: ITO/POx-TPACz/PEDOT:PSS/PVK:PBD:Ir(Cz-ppy)$_3$/TAZ/Alq$_3$/Lif/Al.

For multilayer devices, 3-(biphenyl-4-yl)-5-(4-*tert*-butylphenyl)-4-phenyl-4H-1,2,4-triazole (TAZ) and tris(8-hydroxy-quinoline) aluminium (Alq$_3$) layer were vacuum-deposited onto the emitting polymer layer. Finally, LiF (1 nm)/Al (100 nm) electrodes were deposited onto the Alq$_3$ layer. Current–density–voltage characteristics were measured with a Keithley 2400 source meter. The brightness and electroluminscence spectra of the devices were measured with Spectra Colorimeter PR-650.

3. Results and discussion

3.1. Synthesis of photoreactive main chain conjugated polymer bearing oxetane moieties in the side chain (POx-TPACz)

A simple synthetic rout to the photoreactive polymer, Pox-TPACz is shown in Scheme 1.
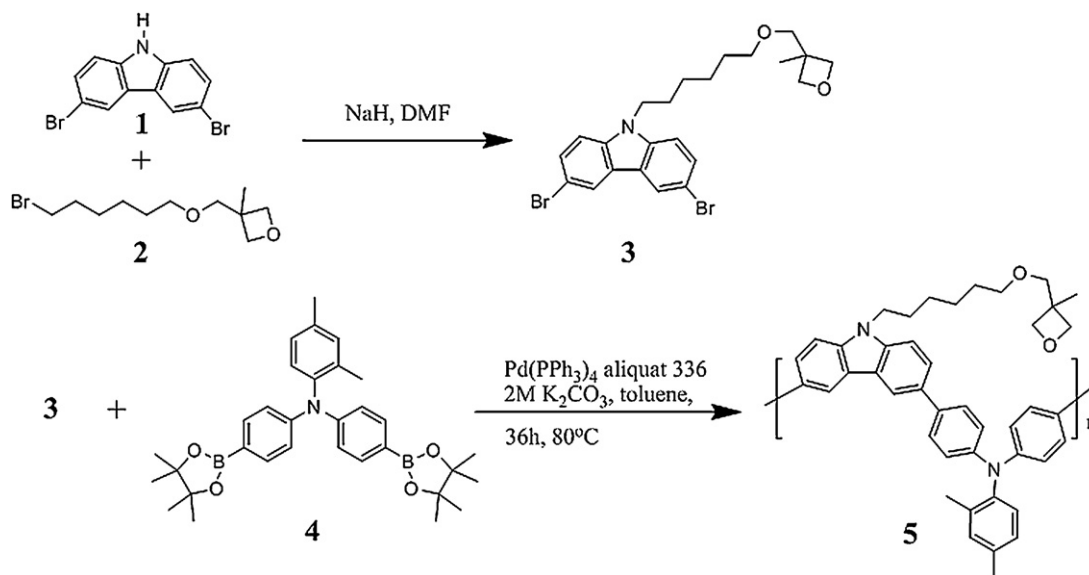
Scheme 1. Synthetic procedure for photoreactive main chain conjugated polymer.
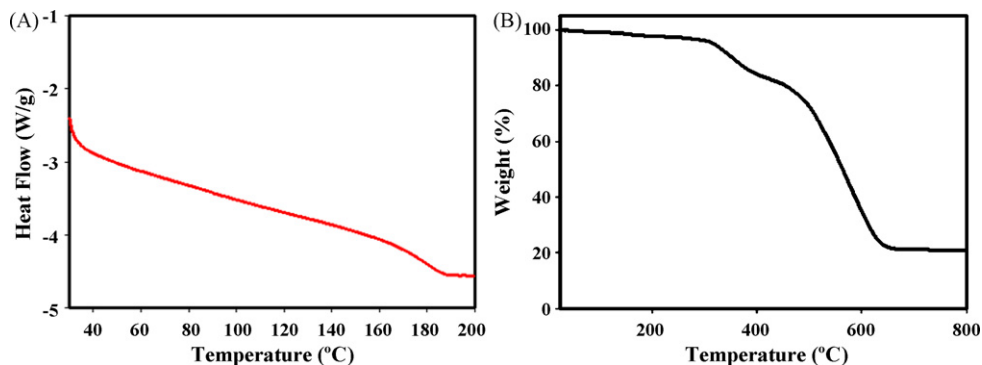

Fig. 1. DSC (A) and TGA (B) thermograms of POx-TPACz.

3,6-Dibromo-9*H*-carbazole and 3-((6-bromohexyloxy)methyl)-3-methyloxetane were prepared according to the method given in the literature [24]. The substitution reaction of 3-((6-bromohexyloxy)methyl)-3-methyloxetane into 3,6-dibromo-9*H*-carbazole yields 3,6-dibromo-9-(6-((3-methyloxetan-3-yl)methoxy)hexyl)-9*H*-carbazole (**3**) in the presence of sodium hydride. The polymerization of **3** and 2,4-dimethyl-*N,N*-bis(4-(4,4,5,5-tetramethyl-1,3,2-dioxaborolan-2-yl)phenyl)aniline (**4**) was performed by the Suzuki coupling reaction with a yield of 85%. The resulting material was then purified by Soxhlet extraction with methanol. The identities of the synthetic compounds were confirmed by proton nuclear magnetic resonance (^{1}H NMR). The resulting polymer was found to have a good self-film forming property and was well soluble in various organic solvents such as chloroform, xylene, methylenechloride, monochlorobenzene, and tetrahydrofuran.

The thermal properties of the polymer were characterized by differential scanning calorimetry (DSC) and thermogravimetric analysis (TGA). DSC measurement was performed at a heating (cooling) scan rate of $10\,(-10)\,°$C/min under nitrogen with the highest temperature limited to below the decomposition temperature. The polymer exhibits no distinct crystalline-isotropic transitions in the range of 25–220 °C, but shows clear glass transition temperatures ($T_g^{onset} = 165\,°$C). The cationic photocross-linking reaction was performed in the vicinity of the T_g.

TGA measurements at a heating rate of 10 °C/min under nitrogen revealed that the polymers had good thermal stabilities and enhanced onset decomposition temperatures ($\sim$300 °C). The aliphatic chains between the main chain backbone and the side chain oxetane moiety in the polymer were relatively weak against thermal energy (Fig. 1).
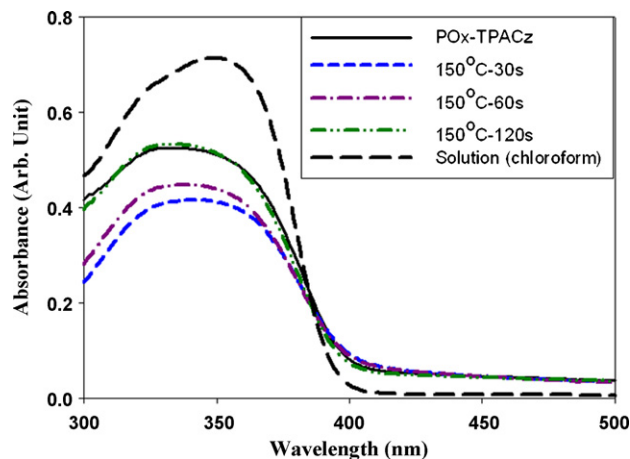

Fig. 2. UV–vis absorption spectra of the film samples before and after photo-curing under 254 nm UV light. The spectra were obtained after rinsing the photo-cured films in monochlorobenzene.
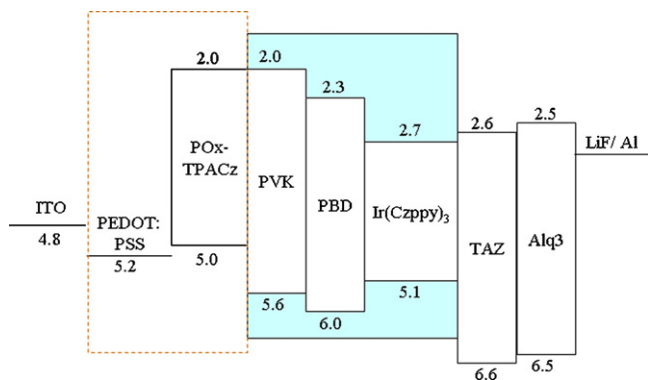
Fig. 3. Energy band alignment in the electrophosphorescence devices.

Fig. 5. Dependence of current density and luminance on the applied voltage. *Open symbol*: luminance; *filled symbol*: current density. *Inset*: the electroluminescent EL spectra of four devices.

3.2. UV–vis absorption behavior of POx-TPACz

The absorption spectra of the samples of POx-TPACz in solution and film states are shown in Fig. 2. The solution and film samples exhibit absorption bands at 300–400 nm. The absorption bands of the spectra are ascribed to the π–π^* transitions originating from the conjugated polymer backbone.

The solubility change of the film before and after photo-curing was investigated. The film was rinsed with monochlorobenzene after UV irradiation under a fixed irradiation time and the spectra were again recorded (e.g., 30, 60, and 120 s at 150 °C).

After 30 and 60 s curings, the samples showed decrement of absorbance due to partial dissolution. However, the film cured under 120 s UV exposure showed no decrement of absorbance, indicating that it was highly resistant to the solvent.

Using cyclic voltammetry (CV), the oxidation potential of POx-TPACz was measured to be 0.66 V. The HOMO level of POx-TPACz was determined to be almost -5.06 eV. In order to determine the lowest unoccupied molecular orbital (LUMO) level, the oxidation potential from the CV was combined with the optical energy bandgap (E_g) resulting from the absorption edge in the absorption spectrum. The LUMO level of POx-TPACz was determined to be -2.00 eV.

3.3. Electrophosphorescence of multilayered devices

Multilayered diodes are structured as ITO/(HIL and/or HTL)/PVK: PBD with Ir(Cz-ppy)$_3$ (40 nm)/TAZ (10 nm)/Alq$_3$ (30 nm)/LiF

(0.8 nm)/Al (80 nm) (see Fig. 4). Four different multilayered electrophosphorescent devices (A–D) were fabricated using a different layered structure in the hole injection/transport layer. In Fig. 3, the energy level alignment of all of the layers comprising the PLEDs can be seen. It should be noted that the HOMO level of POx-TPACz is slightly lower than that of PEDOT:PSS (Fig. 3).

The devices were fabricated by doping Ir(Cz-ppy)$_3$ (10 wt.%) into a PVK:PBD (70:30 wt. ratio) host. Due to steric hindrance by the carbazole groups, these complexes can be employed in devices at high concentrations without incurring significant concentration quenching of the photoluminescence (PL). There is a good overlap between the PL spectrum of PVK or PVK:PBD (30 wt.%) and the metal-ligand charge transfer (MLCT) absorption bands of iridium complexes [8,26]. This overlap should enable efficient energy transfer from the singlet-excited state in the host to the MLCT band of the guest. Detailed device performance is summarized in Table 1.

The current density–voltage luminance curves of the four devices are shown in Fig. 5. Turn-on voltages for these devices are typical for Ir(III) complex-doped PLEDs, falling in the 6.0–6.5 V range. The higher turn-on voltage of 6.5 V might be attributed to the dielectric nature of the cross-linked POx-TPACz. The lower current at a fixed applied voltage in devices C and D is due to the poor hole injection/interfacial property through the cured POx-TPACz. Among all devices, device D had the maximum brightness of around 31,000 cd/m^2 (at 198.01 mA/cm^2) and it was comparable to that of device A.
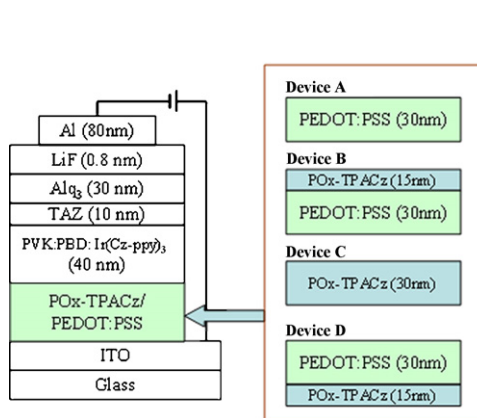

Fig. 4. The device configurations of electrophosphorescent PLEDs. Molecular structures of Ir(Cz-ppy)$_3$, PVK, TAZ, POx-TPACz, PBD and cationic photoinitiator.
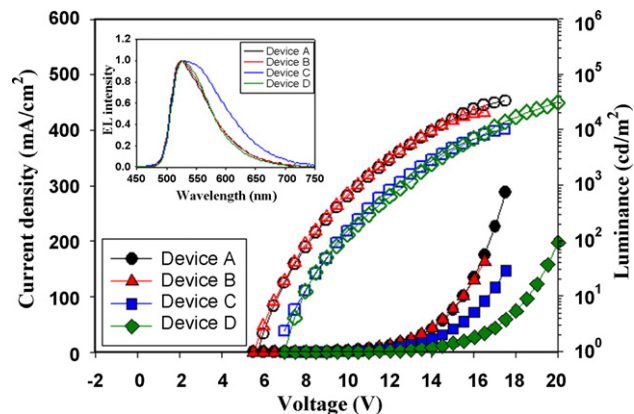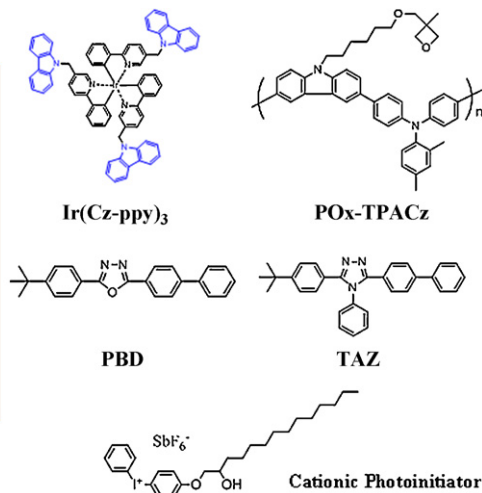
Table 1
Measured parameters of electrophosphorescent devices.

| Device	Turn-on (V)	Max. luminance/cd m^{-2} (corresponding J)	Max. luminous efficiency/cd A^{-1} (corresponding J)	Max. power efficiency/lm W^{-1} (corresponding J)	Max. external quantum efficiency/η_{ext} (corresponding J)
A	5.5	32,970 (288.24), at 17.5 V	25.39 (3.74), at 10.5 V	7.59 (3.74), at 10.5 V	8.11 (3.74), at 10.5 V
B	5.5	20,050 (163.22), at 16.5 V	24.36 (6.05), at 11 V	8.55 (0.38), at 8 V	7.68 (2.79) at 10 V
C	7.0	10,930 (222.18), at 18.5 V	12.47 (4.67), at 11.5 V	3.40 (4.67), at 11.5 V	4.38 (4.67), at 11.5 V
D	7.0	31,000 (198.01), at 20 V	28.18 (11.3), at 14.5 V	7.74 (0.51), at 10 V	8.73 (1.58), at 11.5 V
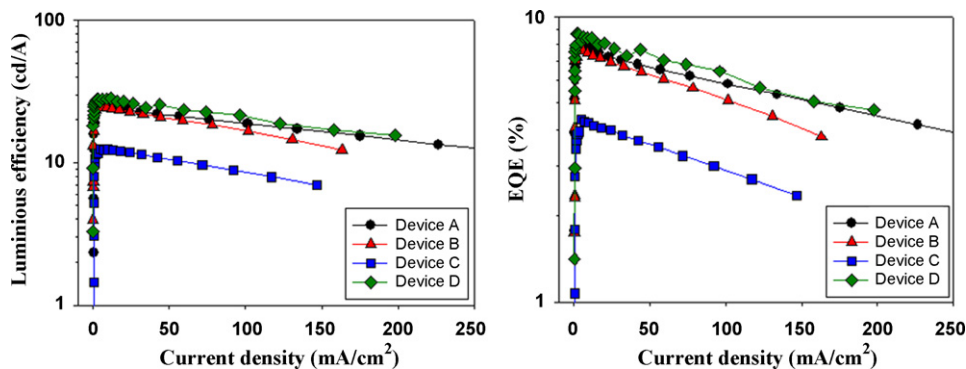
Fig. 6. Dependence of luminous efficiency and external quantum efficiency on the current density.

When the POx-TPACz layer was deposited on PEDOT:PSS, hole transport through the layers was difficult due to misalignment of the HOMO levels of PEDOT:PSS and POx-TPACz. In contrast, the performance of the devices improved when a POx-TPACz layer was inserted between the ITO and PEDOT:PSS layers. The HOMO level of POx-TPACz is slightly lower than that of PEDOT:PSS; therefore, the holes can be easily transported in a gradient energy pathway and this allows the holes to be injected into green emitting electrophosphorescent devices.

Device C showed the lowest brightness at around 10,930 cd/m^2, which was one-third that of device A (L_{max} = 32,970 cd/m^2), due to the fact that device C showed only broader electroluminescence spectra, changing the color coordinates, which strongly govern device efficiency and other performances (see inset of Fig. 5).

Fig. 6 shows the dependence of the luminous efficiency and external quantum efficiency on the current density for the four devices. The doping of PBD into PVK can be attributed to the fact that electron transport was highly facilitated to exhibit balanced emission in the emission layer. Well-balanced charge-carrier injection and transport and confinement of the emissive triplet excitons within the emission layer were achieved, resulting in significantly improved device efficiency.

The maximum luminous efficiency of device D was determined as 28.18 cd/A (at 11.3 mA/cm^2, η_{EQE} = 8.73% at 1.58 mA/cm^2), which is slightly higher than that of even device A. When the cross-linked POx-TPACz was used as the hole injection interlayer on the ITO anode with the PEDOT:PSS layer, the brightness and efficiency was slightly improved.

Both light output and quantum efficiency in device D demonstrate that the utilization of a bilayered HIL/HTL structure with better matched HOMO levels improved the efficiency of hole injection from POx-TPACz/PEDOT:PSS to the PVK-based emitting layer. Due to the presence of a carbazolyl peripheral moiety, the present device has a slower decrease in efficiency with an increase in current density, thereby suppressing triplet–triplet annihilation.

Although the single HIL of cross-linked POx-TPACz demonstrated poor efficiency in device C due to spectral broadening, the combination of PEDOT:PSS and POx-TPACz displayed some promising experimental results.

Finally, it should be emphasized that the surface property of cured POx-TPACz is quite compatible with that of PEDOT:PSS and the ITO layer. Significant wetting of the cross-linked POx-TPACz structure containing 2-methylpropylene oxide was exhibited on top and underneath PEDOT:PSS. The compatibility between the PEDOT:PSS layer and the cured POx-TPACz also significantly affected the device characteristics and reproducibility.

4. Conclusions

The study herein demonstrated a new hole transport or injection layer, which facilitates hole injection/transport properties and result in well-balanced charge recombination in the emitting layer. The hydrophilic nature of the 2-methylpropylene oxide in the structure of cross-linked POx-TPACz aided compatibility with the PEDOT:PSS and the ITO layer. In particular, the efficiency of device D (ITO/POx-TPACz/PEDOT:PSS/Ir(ppy-Cz)$_3$ in PVK:PBD/TAZ/Alq$_3$/LiF/Al) is better than that of the other conventional devices. Conventional phosphorescent PLEDs are focused on the device configuration using PEDOT:PSS only. Cascade HOMO energy alignment helps to improve the hole transporting property and the solvent resistance of HIL using the photocross-linkable interlayer. Our study unambiguously describes a new POx-TPACz interlayer that takes advantage of efficient hole transport and solvent resistance. It can be fully utilized for fabricating better solution processed phosphorescent EL devices.

References

[1] C. Adachi, M.A. Baldo, M.E. Thompson, S.R. Forrest, J. Appl. Phys. 90 (2001) 5048.
[2] A.P. Wilde, K.A. King, R.J. Watts, J. Phys. Chem. 95 (1991) 629.
[3] S. Bernhard, J.A. Barron, P.L. Houston, H.D. Abruña, J.L. Ruglovksy, X. Gao, G.G. Malliaras, J. Am. Chem. Soc. 124 (2002) 13624.
[4] T. Tsutsui, M.-J. Yang, M. Yahiro, K. Nakamura, T. Watanabe, T. Tsuji, Y. Fukuda, T. Wakimoto, S. Miyaguchi, Jpn. J. Appl. Phys. 38 (1999) L1502.

[5] J.C. Ostrowski, M.R. Robinson, A.J. Heeger, G.C. Bazan, Chem. Commun. (2002) 784.
[6] J.P. Duan, P.P. Sun, C.H. Cheng, Adv. Mater. 15 (2003) 224.
[7] A. Beeby, S. Bettington, I.D.W. Samuel, Z. Wang, J. Mater. Chem. 13 (2003) 80.
[8] X. Gong, M.R. Robinson, J.C. Ostrowski, D. Moses, G.C. Bazan, A.J. Heeger, Adv. Mater. 14 (2002) 581.
[9] M. Ikai, S. Tokito, Y. Sakamoto, T. Suzuki, Y. Taga, Appl. Phys. Lett. 79 (2001) 156.
[10] Q. Huang, J. Li, G.A. Evmenenko, P. Dutta, T.J. Marks, Chem. Mater. 18 (2006) 2431.
[11] Q. Huang, G. Evmenenko, P. Dutta, T.J. Marks, J. Am. Chem. Soc. 125 (2003) 14704.
[12] R.A. Hatton, M.R. Willis, M.A. Chesters, D. Briggs, J. Mater. Chem. 13 (2003) 722.
[13] J. Lee, B.-J. Jung, J.-I. Lee, H.Y. Chu, L.-M. Do, H.-K. Shim, J. Mater. Chem. 12 (2002) 3494.
[14] D. Parker, Q. Pei, M. Marrocco, Appl. Phys. Lett. 65 (1994) 1272.
[15] J.H. Gruener, F. Wittmann, P.J. Hamer, R.H. Friend, J. Huber, U. Scherf, K. Muellen, S.C. Moratti, A.B. Holmes, Synth. Met. 67 (1994) 181.
[16] T. Braig, D.C. Müller, M. Gross, K. Meerholz, O. Nuyken, Macromol. Rapid Commun. 21 (2000) 583.
[17] Y.-D. Zhang, R.D. Hreha, G.E. Jabbour, B. Kippelen, N. Peyghambarian, S.R. Marder, J. Mater. Chem. 12 (2002) 1703.
[18] M.S. Bayerl, T. Braig, O. Nuyken, D.C. Müller, M. Gross, K. Meerholz, Macromol. Rapid. Commun. 20 (1999) 224.
[19] S. Liu, X. Jiang, H. Ma, M.S. Liu, A.K.-Y. Jen, Macromolecules 33 (2000) 3514.
[20] X. Jiang, S. Liu, M.S. Liu, P. Hergurth, A.K.-Y. Jen, H. Fong, M. Sarikaya, Adv. Funct. Mater. 12 (2002) 745.
[21] L.D. Bozano, K.R. Carter, V.Y. Lee, R.D. Miller, R. DiPietro, J.C. Scott, J. Appl. Phys. 94 (2003) 3061.
[22] M.-Y. Chou, M.-K. Leung, Y.O. Su, C.L. Chiang, C.-C. Lin, J.-H. Liu, C.-K. Kuo, C.-Y. Mou, Chem. Mater. 16 (2004) 654.
[23] M.J. Cho, J.I. Kim, C.S. Hong, Y.M. Kim, Y.W. Park, B.-K. Ju, D.H. Choi, J. Polym. Sci. Polym. Chem. 46 (2008) 7419.
[24] Y.-K. Yun, D.-H. Ko, J.-I. Jin, Y.S. Kang, W.-C. Zin, B.-W. Jo, Macromolecules 33 (2000) 6653.
[25] O. Solomeshch, V. Medvedev, P.R. Mackie, D. Cupertino, A. Razin, N. Tessler, Adv. Funct. Mater. 16 (2006) 2095.
[26] H.-M. Liu, J. He, P.-F. Wang, H.-Z. Xie, X.-H. Zhang, C.-S. Lee, B.-Q. Sun, Y.-J. Xia, B.-Q. Sun, Y.-J. Xia, Appl. Phys. Lett. 87 (2005) 221103.